Optimization and experimental analysis of sweet potato ship-shaped transplanting trajectory using particle swarm algorithm

Zhengduo Liu[1,2], Lin Hua[1], Zhaoqin Lyu[3], Jiaji Hu[4], Wenxiu Zheng[3*]

(1. *College of Mechanical and Vehicle Engineering, West Anhui University, Lu'an 237000, Anhui, China*;
2. *Traditional Chinese Medicine Institute of Anhui Dabie Mountain, West Anhui University, Lu'an 237012, Anhui, China*;
3. *College of Mechanical and Electronic Engineering, Shandong Agricultural University, Tai'an 271018, Shandong, China*;
4. *Anhui Zhengyang Machinery Technology Co., Ltd., Lu'an 237012, Anhui, China*)

Abstract: The mechanization of ship-shaped transplanting is currently an urgent problem that should be solved. The movement trajectory of the transplanting mechanism is the key technology to perform ship-shaped transplanting. In this study, a ship-shaped transplanting trajectory was built and a mathematical model of a four-link transplanting mechanism was developed based on the requirements of the sweet potato transplanting agronomic technology. The particle swarm optimization algorithm was used, with the length of the four-bar mechanism and the installation angle of the fixed bar serving as the variables to optimize. The objective was to minimize the deviation of the ship-shaped transplanting trajectory, yielding an iterative optimization solution. The MATLAB simulation results showed that the penalty factors of different proportions in the adaptive particle swarm optimization algorithm affected the transplanting trajectory. The optimal penalty factor parameters are α=0.6, β=0.4. They ensure that the transplanting trajectory fulfills the agronomic requirements, and limit the deviation in the return trajectory of the mechanism. The sizes of the optimized four-bar mechanism were 110, 312, 245, 160, 360, and, 160 mm. The determined installation angle was 100°. The results of the field experiments demonstrated that the optimized four-bar transplanting mechanism can better fulfill the agronomic technical requirements of sweet potato ship-shaped transplanting. For a transplanting speed of 0.2 m/s, the average qualified rates of insertion depth, insertion length, and tail height were equal to 94.00%, 93.83%, and 91.67%. The results obtained in this study provide a theoretical basis and technical support for studying and developing sweet potato ship-shaped transplanting machinery.

Keywords: sweet potato, oblique insertion method, mechanical arm, particle swarm
DOI: 10.25165/j.ijabe.20241703.8201

Citation: Liu Z D, Hua L, Lyu Z, Hu J J, Zheng W X. Optimization and experimental analysis of sweet potato ship-shaped transplanting trajectory using particle swarm algorithm. Int J Agric & Biol Eng, 2024; 17(3): 100–107.

1 Introduction

Transplanting is still a challenge in the industrialization of sweet potatoes[1,2]. Due to the decrease of the agricultural population in China, the transplanting has become a major force in its agricultural production. Therefore, the development of a machine suitable for transplanting sweet potato seedlings served as the development orientation of potato-related machines for a certain period in China[3,4].

In developed nations, such as Europe and the United States, most of the sweet potato seedlings are transplanted by large machinery[5,6]. The American Machinery Company has produced a semi-automatic chain clip-type transplanter for the oblique insertion of bare-rooted sweet potato seedlings, which is drawn by a large-horsepower tractor. Although this transplanter has high transplanting efficiency, it is unable to fulfill the technical requirements for ship-shaped transplanting. More precisely, the seedlings are vertically inserted into the soil at their roots, while a section of seedlings is horizontally laid out and buried in the surface layer of the soil. In addition, seedlings with leaves are positioned outside the soil. The overall arrangement of the seedlings resembles the shape of a boat shape. In many countries, including Japan, small transplanters are universally applied. A company in the Henan Province of China imported two sets of self-propelled sweet potato transplanters from Japan. This machine is based on a clip-type oblique insertion method. However, this was not applicable to the ship-shaped transplanting of sweet potato seedlings, and it has a high cost. In China, studies on such transplanters have been recently emerged, while the general transplanters remained the objects of most of the studies[7,8]. In recent years, several studies have been conducted on a unique transplanter for sweet potatoes in China. For instance, the Shanxi Academy of Agricultural Sciences developed a simple transplanter which is able to simultaneously punch, water, and transplant seedlings. However, this machine requires manual transplanting and does not allow the mechanical transplanting. A study[9] surveyed sweet potato transplanting, and adopted a flexible chain clip-type transplanter to directly and obliquely transplant sweet potato seedlings. A 2ZGF-2 compound sweet potato transplanter was also developed[10]. This transplanter can transplant sweet potatoes through oblique insertion for two ridges at once. The aforementioned studies demonstrated that the direct and oblique insertions are the main mechanical sweet potato transplanting methods used in China. A study also explored the mathematical

Received date: 2023-02-21 **Accepted date:** 2024-02-28
Biographies: Zhengduo Liu, PhD, Lecturer, research interest: intelligent agricultural machinery equipment, Email: 1362825417@qq.com; **Lin Hua**, PhD, Associate Professor, research interest: mechanical automation, Email: 114935390@qq.com; **Zhaoqin Lyu**, PhD, Professor, research interest: intelligent agricultural machinery equipment, Email: 1535446029@qq.com; **Jiaji Hu**, Engineer, research interest: intelligent agricultural machinery equipment, Email: ahzenyi@163.com.

***Corresponding author: Wenxiu Zheng**, PhD, Lecturer, research interest: intelligent agricultural machinery equipment. College of Mechanical and Electrical Engineering, Shandong Agricultural University, Tai'an 27100, Shandong, China. Tel: +86-15094808087, Email: 15094808087@163.com.

description of the link curves of a plane four-bar mechanism in the frequency domain, aiming at optimizing the trajectory[11]. The link curves were established with numerical mapping using the Fourier series, which solved the comprehensive trajectory problem of the mechanism. In other studies[12,13], the four-bar mechanism was optimized using power functions. The ADAMS dynamic simulation software was used for the modeling and trajectory simulation of the four-bar mechanism[14-16]. Note that the studies presented in this literature review provided a foundation and a theoretical basis for the study conducted in this study.

The sweet potato ship-shaped transplanting has high yield, small size difference, and decent commodity properties compared with the straight and oblique transplanting, which is favored by potato farmers. However, to the best of our knowledge, a mature ship-shaped transplanting machinery on the market at present does not exist. The existing ones require manual transplanting with high labor intensity and low efficiency. The mechanization of the ship-shaped transplanting is an urgent problem in sweet potato planting and production. The trajectory of the ship-shaped transplanting is also a problem. A previous study tackled the oblique planting technology of sweet potatoes[17,18], which effectively addressed the issue of oblique insertion during transplantation. Based on this study, this paper adopts a four-bar linkage as the ship-shaped transplanting mechanism, and uses the particle swarm optimization algorithm[19-22] to optimize and address challenges related to trajectory and mechanism design in sweet potato ship-shaped transplantation.

2 Materials and methods

2.1 Agrotechnical requirements

According to the agrotechnical requirements for the ship-shaped transplanting of sweet potatoes, the ship-shaped manual transplanting trajectory was simulated in the present study, and the result is shwon in Figure 1. In this figure, d denotes the insertion depth, which ranged from 50 to 70 mm, l denotes the insertion length, which ranged from 150 to 170 mm, and c denotes the tail height, which ranged from 20 to 35 mm.

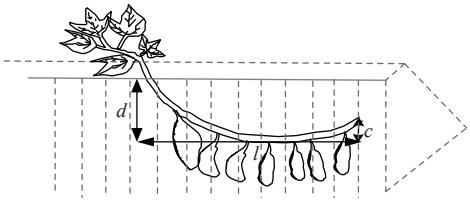

Figure 1 Sweet potato ship-shaped transplanting track

2.2 Mathematical model

A four-bar mechanism was used as the transplanting mechanism for sweet potato seedlings. This mechanism was mathematically modeled, as illustrated in Figure 2. It comprises the *CB* crank, the *OD* rocker, the *BDA* rocker, and the *OC* fixed connecting bar. When the mechanism operates, the crank, which is the driving member, rotates around a fixed axis through point *C*, which drives the *OD* rocker to swing around a fixed axis through point *O*, while the *BDA* rocker is in planar motion. The movement trajectory of endpoint A is referred to as the transplanting trajectory.

The four-bar mechanism *OCBD* was considered a closed vector polygon. Given l_1, l_2, l_3, l_4, l_5 ω, θ, φ, and v, the closed vector equation of the four-bar mechanism is expressed as:

$$l_1 + l_4 = l_2 + l_3 \tag{1}$$

The plural form of the above equation could then be expressed as below:

$$l_1 e^{i\alpha_1} + l_4 e^{i\alpha_4} = l_2 e^{i\alpha_2} + l_3 e^{i\alpha_3} \tag{2}$$

Accordingly, the coordinate of point $A(x',y')$at time t was derived as follows:

$$\begin{cases} x' = X\cos\theta - Y\sin\theta \\ y' = X\sin\theta + Y con\theta \end{cases} \tag{3}$$

where, x' is the abscissa of point A at any time; y' is the ordinate of point A at any given time; $X=x_1+x_2+x_3+vt$; $Y=y_1+y_2+y_3$; $x_1=l_2\cos\omega t$; $y_1=l_1-l_2\sin\omega t$;

$$x_2 = l_3\cos\left(2\arctan\cdot\left(\frac{-2al_3 \pm \sqrt{(-2al_3)^2 + 2bl_3^2 - (l_2^2 + l_1^2 + l_3^2 - l_4^2 - 2l_1l_2\sin\omega t)^2}}{2bl_3 - (l_2^2 + l_1^2 + l_3^2 - l_4^2 - 2l_1l_2\sin\omega t)}\right)\right) \tag{4}$$

$$x_3 = l_5\cos\left(2\arctan\cdot\left(\frac{-2al_3 \pm \sqrt{(-2al_3)^2 + 2bl_3^2 - (l_2^2 + l_1^2 + l_3^2 - l_4^2 - 2l_1l_2\sin\omega t)^2}}{2bl_3 - (l_2^2 + l_1^2 + l_3^2 - l_4^2 - 2l_1l_2\sin\omega t)} + 180 - \varphi\right)\right) \tag{5}$$

$$y_2 = l_3\sin\left(2\arctan\cdot\left(\frac{-2al3 \pm \sqrt{(-2al3)^2 + 2bl_3^2 - (l_2^2 + l_1^2 + l_3^2 - l_4^2 - 2l_1l_2\sin\omega t)^2}}{2bl_3 - (l_2^2 + l_1^2 + l_3^2 - l_4^2 - 2l_1l_2\sin\omega t)}\right)\right) \tag{6}$$

$$y_3 = l_5\sin\left(2\arctan\cdot\left(\frac{-2al_3 \pm \sqrt{(-2al_3)^2 + 2bl_3^2 - (l_2^2 + l_1^2 + l_3^2 - l_4^2 - 2l_1l_2\sin\omega t)^2}}{2bl_3 - (l_2^2 + l_1^2 + l_3^2 - l_4^2 - 2l_1l_2\sin\omega t)} + 180 - \varphi\right)\right) \tag{7}$$

$$a = -l_1 + l_2\sin\omega t,\ b = l_2\cos\omega t \tag{8}$$

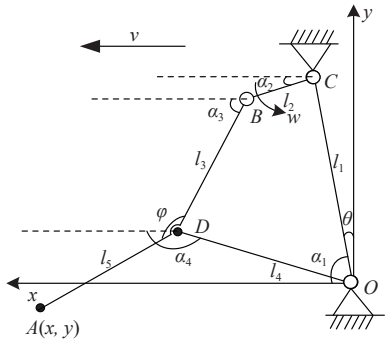

Note: l_1, l_2, l_3, l_4, and l_5 represent the vectors of the bars, mm; α_1, α_2, α_3, and α_4 respectively denote the counterclockwise angles between the positive direction of the x-axis and l_1, l_2, l_3, and l_4, rad; φ denotes the angle between the l_3 and l_5 bars, rad; ω denotes the rotating angular speed of the l_2 crank, rad/s; v denotes the forward speed of the machine, m/s; θ represents the installation angle of the l_1 fixed connecting bar, rad.

Figure 2 Kinematics model of the transplanting mechanism

2.3 Optimization of the transplanting trajectory based on particle swarm optimization

2.3.1 Reference trajectory

In order to apply the particle swarm optimization algorithm to the optimization of the sweet potato transplanting trajectory, the ship-shaped transplanting trajectory shown in Figure 1 is

represented by a series of continuous points using the tracing method, and the trajectory is completed into a closed area by simulating the manual transplanting process, as shown in Figure 3. Note that Q_1 represents the reference trajectory for seedling insertion by the boat-shaped transplanting mechanism. It also determines the shape of the planting trajectory (presented by solid lines). In addition, Q_2 represents the return reference trajectory of the boat-shaped transplanting mechanism (presented by dashed lines).The insertion depth, insertion length, and tail height are 60 mm, 160 mm, and 25 mm, respectively.

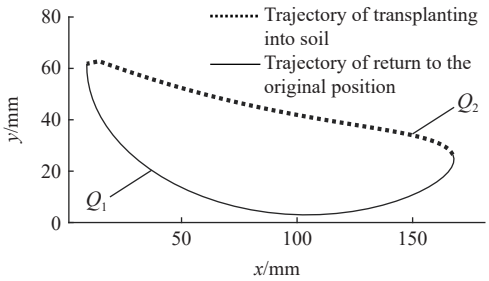

Figure 3 Reference track of the ship-shaped transplanting of sweet potato seedlings

2.3.2 Adaptive PSO algorithm

The bar length of the four-bar mechanism, bending angle of the rocker, and installation angle of the fixed connecting bar were considered as the optimization variables $[l_1, l_2, l_3, l_4, l_5, \theta, \varphi]$. The particles in the PSO algorithm can be adopted to adjust the optimization direction based on their respective optimal solutions as well as those of the swarm. The speed vector was iterated as:

$$v[i] = w_k v[i] + c_1 r_1 \left(\mathrm{pb}[i] - p[i]\right) + c_2 r_2 \left(\mathrm{gb} - p[i]\right) \tag{9}$$

The position vector was iterated as:

$$p[i] = p[i] + v[i] \tag{10}$$

where, c_1 and c_2 are acceleration constants, r_1 and r_2 are random numbers, w_k denotes the inertia weight, $p[i] = [l_1, l_2, l_3, l_4, l_5, \theta, \varphi]$ represents the current solution of the i-th particle, $v[i]$ denotes the speed vector of the i-th particle, pb[i] represents the historical optimal solution of an individual, and gb is the global optimal solution of the particle swarm.

The adaptive weight can then be expressed as:

$$w_k = \left(w_{\min} + \frac{(fit[i] - fit_{\min})(w_{\max} - w_{\min})}{fit_{\mathrm{avg}} - fit_{\min}}\right) \tag{11}$$

where, $fit[i]$ represents the current value of the objective function of the i-th particle, $fit_{\min}$ and fit_{avg} are respectively the minimum and average values of the objective function of the particle swarm.

The constraints for the trajectory optimization of the four-bar mechanism were as follows:

1) The lengths and the rotation angles of the bars

$$\begin{cases} 50\ \mathrm{mm} \le l_1, l_2, l_3, l_4, l_5 \le 1000\ \mathrm{mm} \\ 0 < \alpha_1, \alpha_2, \alpha_3, \alpha_4, \theta, \varphi < \pi \end{cases} \tag{12}$$

2) The mechanisms of the crank and the rocker

$$\begin{cases} l_2 \le l_1;\ l_2 \le l_3;\ l_2 \le l_4 \\ l_3 + l_4 \ge l_1 + l_2;\ l_1 + l_4 \ge l_3 + l_2;\ l_1 + l_3 \ge l_4 + l_2 \end{cases} \tag{13}$$

2.3.3 Objective function

The objective function is the key for optimizing the transplanting trajectory. It should accurately reflect the deviation between the simulated and reference trajectories. The Hausdorff distance[22] was used to evaluate the similarity between the simulated and reference transplanting trajectories. The objective function was then constructed in the process flow, as illustrated in Figure 4.

The solution calculated using the PSO algorithm was substituted into Equation (1) to obtain the simulated transplanting trajectory function, which is expressed as:

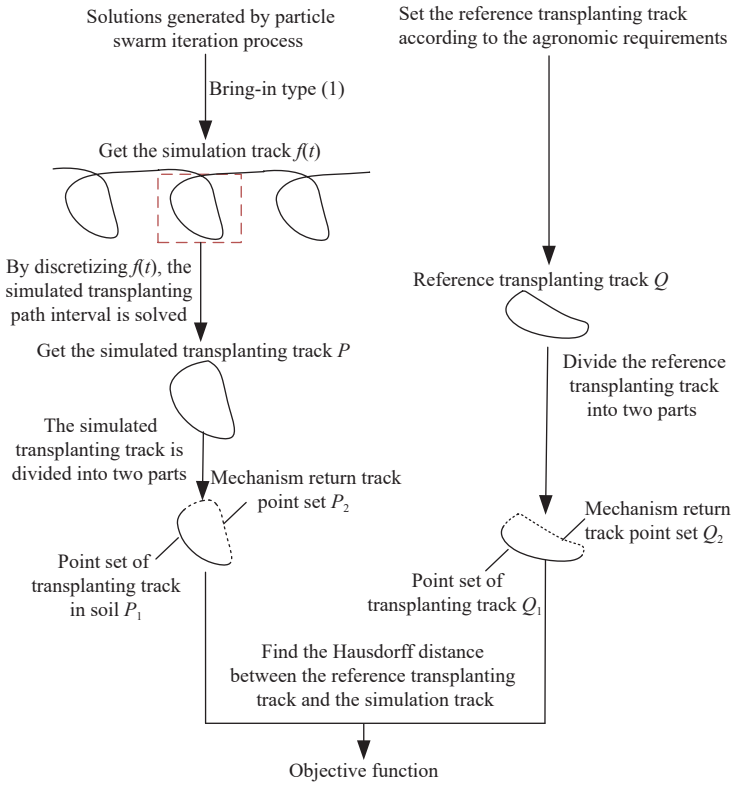

Figure 4 Object function building block diagram

$$\begin{cases} x = g(t) \\ y = f(t) \end{cases} \tag{14}$$

where, $g(t)$ is the parametric equation for the variable x; $f(t)$ is the parametric equation for the variable y.

After discretization, the aforementioned solution was transformed into:

$$\begin{cases} x = \tilde{g}(k) \\ y = \tilde{f}(k) \end{cases} \tag{15}$$

where, k is a discrete variable.

The simulated transplanting trajectory interval $[k_1, k_2]$ was resolved as:

$$\begin{cases} \tilde{f}(k_1) = \tilde{f}(k_2) \\ k_1, k_2 \in [0, T] \end{cases} \tag{16}$$

where, k_1 represents the minimum value of the discrete points of the transplantation trajectory, mm; k_2 represents the maximum value of the discrete points of the transplantation trajectory, mm.

Accordingly, the point set P of the simulated transplanting trajectory was expressed as:

$$P \in \{(x,y) | y = \tilde{f}(k), x = \tilde{g}(k), k \in [k_1, k_2]\} \tag{17}$$

The point set P_1 of the simulated transplanting trajectory and the point set P_2 of the simulated returning trajectory of the mechanism were then solved as:

$$\begin{cases} k_1 \le k_{\min} \le k_{\min} \le k_2 \\ k_{\min} = \min(\tilde{g}(t)) \\ k_{\max} = \max(\tilde{g}(t)) \\ t_{\min} = \tilde{g}^{-1}(k_{\min}) \\ t_{\max} = \tilde{g}^{-1}(k_{\max}) \end{cases} \tag{18}$$

$$\begin{cases} P_1 \in \{(x,y) | y = \tilde{f}(k), x = \tilde{g}(k), k \in [k_1, t_{\max}]\} \\ P_2 \in \{(x,y) | y = \tilde{f}(k), x = \tilde{g}(k), k \in [t_{\max}, k_2]\} \end{cases} \tag{19}$$

Finally, the objective function was obtained:

$$J = \alpha \sum \min_{c_1 \in P_1} \|c_1 - c_2\| + \beta \sum \min_{d_1 \in P_2} \|d_1 - d_2\| \{c_2 | c_2 \in Q_1\}, \{d_2 | d_2 \in Q_2\} \tag{20}$$

where, α and β denote the penalty factors.

The first part of the objective function represents the similarity between the reference and the simulated transplanting trajectories in the insertion process. Its second part represents the similarity between the reference and the simulated transplanting trajectories in the returning process. In the PSO algorithm, the transplanting trajectory was divided into two parts, and the penalty factors were introduced into the function. This allowed to enhance the objective function in order to optimize the transplanting trajectory of the sweet potato seedlings.

Since the forward speed of the transplanter is restricted by the manual seedling splitting speed, its simulation parameters were set according to the manual seedling splitting speed and the row spacing of sweet potato transplanting. More precisely, a forward speed (v) of 0.2 m/s and a rotation speed (ω) of 0.8 rad/s were considered with the number of points in the transplanting trajectory plotted using the point depiction method (P_1 = [0, 35) and Q_1 = [0, 35)), the number of points in the returning trajectory plotted using the point depiction method (P_2 = [35, 70) and Q_2 = [35, 70)), $w_{\min}$ = 0.01, and $w_{\max}$ = 2. In order to study the impact of the penalty factors of the objective function on the sweet potato transplanting trajectory, three groups of penalty factors were developed and used in the simulation experiment performed in the MATLAB software. The parameters of the penalty factors were[23-27]: (1) α = 0.5 and β = 0.5; (2) α = 0.6 and β = 0.4; (3) α = 0.7 and β = 0.3. The adopted PSO algorithm framework can be summarized as:

Step 1: The swarm is initialized and the maximum number of iterations is set;

Step 2: The speed and the position vectors of each particle are renewed using Equations (4) and (5), respectively;

Step 3: Equation (7) is used to evaluate whether the renewed vectors of the particles satisfy the constraints for the length and rotation angle of the four bars. If this is not the case, the extreme value of the bar length is selected to fulfill the constraints;

Step 4: Equation (8) is used to evaluate whether the particles fulfill the constraints for the crank and the rocker. If this is not the case, the values of the longest and shortest bars are adjusted to fulfill the constraints;

Step 5: The renewed and resolved parameters of the particles are substituted into the objective function of Equation (15) and the *Pbest* [*i*] and *gbest* values are renewed;

Step 6: It the number of iterations reached the maximum value, *gbest* is output. Otherwise, continuous iterations are performed and step 2 is repeated.

The results of the simulation experiment are presented in Figure 5, Figure 6, and Table 1.

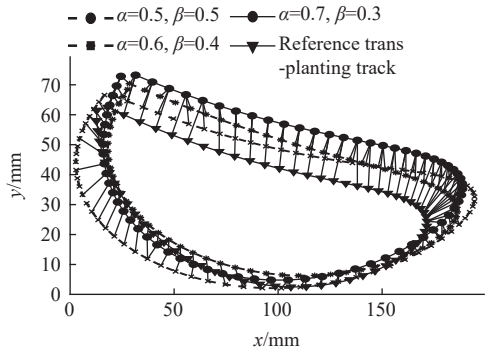

Figure 5 Hausdorff distance of the transplanting trajectory/

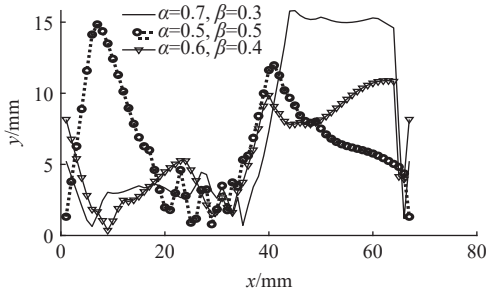

Figure 6 Corresponding point distance

Table 1 Mean of trajectory deviation

	Mean deviation of transplanting trajectory/mm	Mean deviation of trajectory error returned by the transplanting system/mm
1	6.00	7.12
2	3.27	8.58
3	2.92	12.17

It can be seen from Figures 5 and 6 that, when the proportion of the insertion trajectory in the penalty factors increases, the deviation of the insertion trajectory decreases while that of the returning trajectory increases. Therefore, it can be deduced that the penalty factors significantly affect the transplanting trajectory. It can be

seen from Table 1 that in the first group, the insertion trajectory deviation is different by just 1.12 mm compared with the returning trajectory deviation. In the second and third groups, the insertion trajectory deviations are respectively 3.27 mm and 2.92 mm, while the returning trajectory deviations are 8.58 mm and 12.17 mm, respectively. The insertion trajectories of the two groups are consistent, which satisfies the setting of the simulation parameter (i.e., $\alpha \geq \beta$). Since the sweet potato transplanting state depends on the insertion trajectory, α=0.6 and β=0.4 are the preferred parameters for the penalty factors. Moreover, the simulated manual transplanting trajectory is not identical to the kinematics characteristics of the four-bar mechanism, which results in the difference between the reference and simulated transplanting trajectories. The simulated optimal transplanting trajectory of sweet potato seedlings is shown in Figure 7.

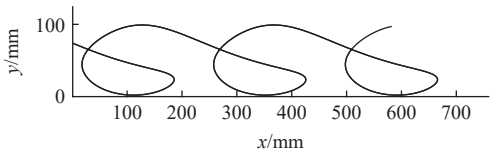

Figure 7 Transplanting trajectory of the adaptive particle swarm optimization algorithm

The parameters of the four-bar mechanism, optimized using the PSO algorithm, are: l_1=360 mm, l_2=110 mm, l_3=312 mm, l_4=245 mm, l_5=160 mm, θ=100º, and φ=160º.

2.3.4 Transplanting trajectory simulation

The parameters of the four-bar mechanism optimized using the PSO algorithm were used to develop a three-dimensional model of the transplanting mechanism in the SolidWorks software. Motion analysis was then conducted to simulate and verify the transplanting mechanism. The simulation results are presented in Figure 8.

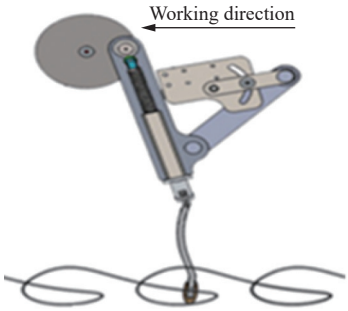

Figure 8 Transplanting trajectories in motion analysis

The trajectory data obtained from the motion analysis were input into MATLAB, which generated the dimensions of the sweet potato transplanting trajectory, as shown in Figure 9. More precisely, the insertion depth, insertion length, and tail height were 63.87, 167.84, and 22.55 mm, respectively. These results showed that the optimized transplanting trajectory fulfills the agrotechnical requirements of the ship-shaped transplanting trajectory for sweet potato seedlings.

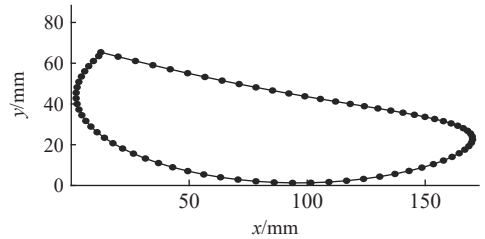

Figure 9 Size of the sweet potato transplanting track

3 Field experiment

3.1 Design of the experimental equipment

In order to verify the actual transplanting trajectory, the experimental equipment for the ship-shaped transplanting mechanism was designed using the optimized geometrical parameters of the four-bar mechanism.

3.1.1 Structural design of the experimental equipment

The designed experimental equipment mainly comprises three parts: the crawler-type chassis, power transmission mechanism, and transplanting mechanism (Figure 10).

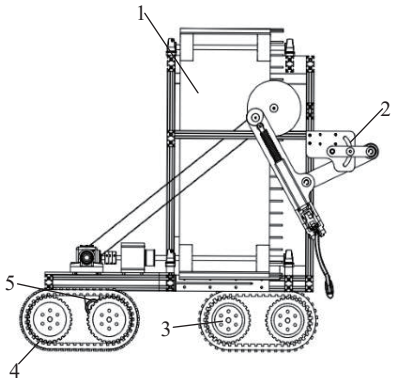

a. Front view

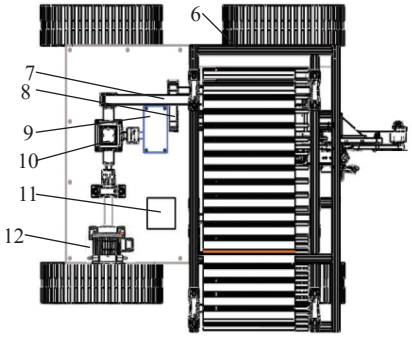

b. Plan view

1. Potato seedling conveyor belt 2. Four bar mechanism 3. Crawler wheel 4. Crawler 5. Chassis motor 6. Baffle 7. Power synchronous belt 8. Synchronous belt of conveyor belt 9. Splitter 10. Transmission 11. STM32 controller 12. Stepper motor

Figure 10 Diagram of the experimental device

In the transplanting process, the seedlings were split and placed in the grooves on the conveyor belt, where they were manually fixed using a hairbrush, as shown in Figure 11. To prevent the seedlings from falling off during the conveying, baffles were mounted onto the sides and the bottom of the conveyor belt and the car frame. A seedling was conveyed to the bottom of the transplanter through the conveyor belt. Afterwards, the grasp fingers of the transplanting mechanism moved to the position of the seedling, grasped it, and then continuously moved until completing the ship-shaped transplanting. The next seedling was then conveyed to the bottom of the transplanter through the conveyor belt, and then grasped and transplanted through the grasp fingers.

3.1.2 Transplanting mechanism

The ship-shaped transplanting mechanism mainly comprises rotating disk, cam, connecting rod, return spring, guide rail, and four-bar mechanism, as shown in Figure 12. The rotating disk (equivalent to a crank), the connecting bar, and the car frame constitute the four-bar mechanism. Using the disk rather than the

crank reduces the shock and the impact of inertia during the crank rotation. When the disk rotates, the roller, under the action of the spring force, remains in touch with the cam. The difference in the radius of the cam causes the spring to be compressed to different extents for controlling the opening and closing of the grasp fingers. The real object of the ship-shaped transplanting mechanism is shown in Figure 13.

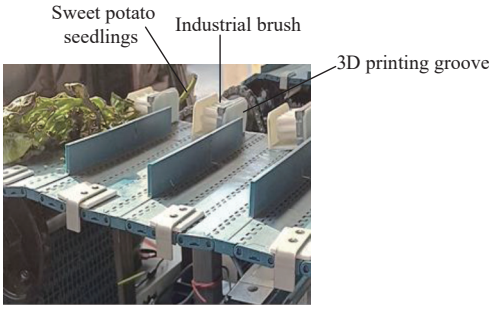

Figure 11 Diagram of fixation of the potato seedling

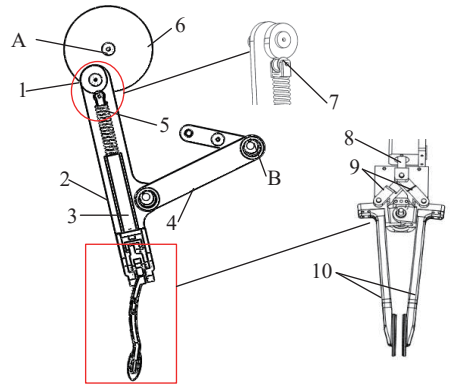

1.Cam 2. Connecting rod 3. Guide rail 4. Connecting rod2 5. Rocker 6. Cam 7. Roller 8. Push rod 9. Fittings 10. Grasp fingers

Note: A is a fixed point of the four-link mechanism; B is another fixed point of the four-link mechanism

Figure 12 Diagram of the transplanting mechanism

Figure 13 Photos of the transplanting mechanism

3.1.3 Power transmission mechanism

The power transmission mechanism comprises the stepper motor, T-type commutator, splitter, synchronous conveyor belt, and power synchronous belt for transplanting. In the transplanting process, after passing through the T-type commutator, the output power of the stepper motor is divided into two paths, as shown in Figure 14a. One of these two power paths allows the power synchronous belt to transplant for driving the mechanism in order to complete the transplanting action. This makes the rotational speed ratio of the stepper motor and the transplanting mechanism equal to 1:1. The other power path allows the splitter to drive the seedling conveyor belt. This makes the rotational speed ratio of the stepper motor and the seedling conveyor belt equal to 1:4. In other words, when the seedling conveyor belt rotates for 1/4th of a round, the seedling on the belt moves forward by one unit of row spacing. When the transplanting mechanism rotates for one complete round, one cycle of transplanting is completed.

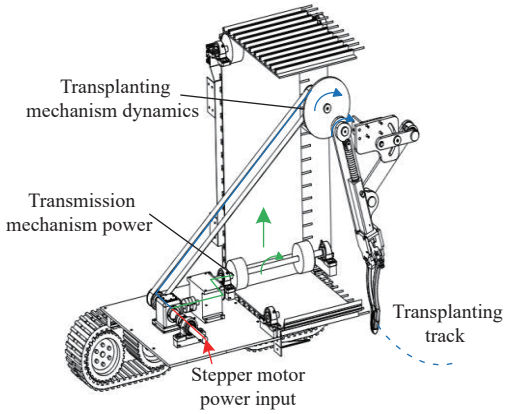

a. Power transmission diagram

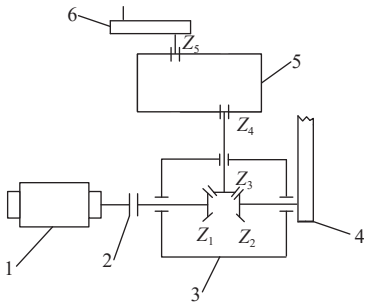

b. Power transmission roadmap

1. Stepping motor 2. Coupling 3. T-type commutator 4. Transplanting machine power synchronous belt 5. Intermittent splitter 6. Transmission synchronous belt

Note: Z_1-Z_5 are transmission wheels at all the levels

Figure 14 Schematic diagram of the power transmission

The power transmission mechanism requires regulating the relationship between the forward and rotational speeds of the transplanting mechanism in order to ensure the transplanting at the set row spacing. The STM32 controller is then used to regulate the rotational speed (ω) of the transplanting mechanism in time based on the forward speed (v) sent by the encoder, such that the transplanter operates at the set row spacing. This yields the following relationship:

$$\omega = \frac{\pi v}{l} \tag{21}$$

where, l denotes the row spacing of sweet potato seedlings, mm; v denotes the transplanter operating speed, m/s; ω denotes the rotational speed of the transplanting mechanism, rad/s. In this study, l=250 mm. Therefore, if v is equal to 0.2 m/s, the derived value of ω is 0.8 rad/s.

Moreover, the power transmission mechanism should ensure the coordination between the seedling conveyor belt and the transplanting mechanism, such that the grasp fingers are able to grasp the seedling properly. According to Figure 14b, the power transmission should satisfy the following formula:

$$\frac{z_1^2 z_5}{z_4 z_3 z_2} = \frac{\pi D}{d} \tag{22}$$

where, d denotes the spacing of the seedlings placed on the

conveyor belt, which is equal to 100 mm.

The transmission ratio of the commutator $\left(\frac{z_1}{z_2}=\frac{z_2}{z_3}=1\right)$ is equal to 1:1, while that of the splitter $\left(\frac{z_5}{z_4}=4\right)$ is equal to 1:4. The diameter of the synchronizing wheel (D) is then equal to 127 mm. In addition, the coordination between the seedling conveyor belt and the transplanting mechanism allows the grasp fingers to properly grasp the seedling.

3.1.4 Invariance of the transplanting trajectory

This study ensures the invariance of the transplanting trajectory of sweet potato seedlings at different forward speeds.

The operation speed (v) yields:

$$\begin{cases} t=\frac{l}{v} \\ \omega=\frac{1}{t} \end{cases} \tag{23}$$

where, t is the operation time for transplanting a seedling, s.

The forward speed v_2 (m/s) and rotational speed ω_2 (rad/s) of the transplanting mechanism yield $\frac{v}{\omega}=\frac{v_2}{\omega_2}$. This indicates that the ratio of the forward speed to the rotational speed of the transplanting mechanism should be fixed to ensure the invariance of the transplanting trajectory. The STM32 controller can regulate the rotational speed of the transplanting mechanism based on the forward speed, which is monitored using the encoder, in order to ensure the invariance of the transmission ratio and the seedling transplanting trajectory.

3.2 Experiment Purpose and Conditions

A field experiment (Figure15) was conducted on the ship-shaped transplanting mechanism in the sweet potato planting experimental base of Shandong Agricultural University, in order to verify the actual transplanting effect of the optimized ship-shaped transplanting mechanism and determine the rational forward speed for transplanting. The operation flow of the transplanting mechanism is shown in Figure 16.

Figure 15 Transplanting test

The sweet potato seedlings were planted on ridges having a spacing of 900 mm. The top width, height, and row spacing of the ridge were 300, 240, and 250 mm, respectively. Sandy soil with moderate viscosity was used with the fresh-edible “Yantai sweet potato 25” variety of seedlings, having a length in the range of 300-350 mm and a diameter in the range of 4.8-5.3 mm. Each seedling had 6-10 leaves.

3.3 Results and discussion

The speed of sweet potato transplanting is limited by the manual seedling splitting speed. In the experiment, the insertion depth, insertion length, and tail height of the sweet potato seedlings were used to evaluate the transplanting effect at a forward speed of 0.2 m/s. Every set of 200 seedlings, transplanted using the prototype, was treated as one group. The experiment conducted on each group was repeated 6 times, and the average of all the obtained results was considered as the final result. The experimental results are presented in Figure 17, Tables 2 and 3.

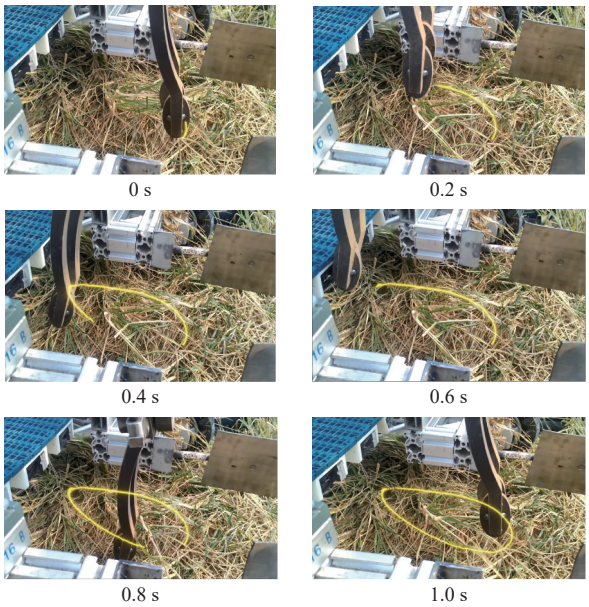

Figure 16 Transplanting mechanism operating diagram

Figure 17 Transplanting track of the ship-shaped transplanting mechanism

Table 2 Transplanting results under different forward speeds

Speed/ m·s^{-1}	Qualified rate of planting depth/%	Qualified rate of seedling length in soil/%	Tail height pass rate/%
0.2	94.0	95.5	92.0
0.2	95.0	93.5	91.0
0.2	93.0	92.5	92.0
0.3	94.0	94.5	91.0
0.3	93.0	93.0	91.0
0.3	93.5	91.0	92.5
0.4	93.0	90.0	91.5
0.4	93.0	91.5	90.0
0.4	92.0	90.0	89.5

Table 3 Test statistics

Item	Speed/m·s^{-1}		
	0.2	0.3	0.4
Average qualified rate of planting depth/%	94.00	93.50	92.67
Mean of the qualified rate of seedling length in soil/%	93.83	92.83	90.50
Tail height pass rate average/%	91.67	91.79	90.33

It can be observed from Tables 2 and 3 that, for a forward speed of 0.2 m/s, the average qualified rates of the insertion depth and length were respectively 94.00% and 93.83%, while that of the tail height was 91.67%. These values fulfilled the agricultural

production standards. In the experiment, it was demonstrated that the seedling roots had significantly different bending forms, which was the underlying cause of the low qualified rate of the tail height of the seedlings. Moreover, the ridge heights were not uniform, which was a key factor affecting the qualified rates of the insertion depth and length. Since a certain distance existed between the grasp fingers and the conveyor belt, seedling leakage would appear in the case of short seedling exposed length. This reduced the qualified transplanting rate to a certain extent.

The insertion depth, insertion length, and tail height of the transplanting trajectory were 65, 167, and 27 mm, respectively. These values fulfill the agrotechnical requirements for the ship-shaped transplanting of sweet potato seedlings.

4 Conclusions

In this study, a reference ship-shaped transplanting trajectory was designed according to the agrotechnical requirements for sweet potato transplanting. A mathematical model was also developed using a four-bar transplanting mechanism.

In addition, the transplanting trajectory of the mechanism was optimized using the adaptive PSO algorithm. The objective trajectory was divided into insertion and returning trajectories. Furthermore, the impact of the various proportions of penalty factors on the ship-shaped transplanting trajectory was studied. In particular, the insertion trajectory was optimized by establishing the penalty factors.

Finally, the results obtained by simulation and field experiments demonstrated that the proposed four-bar transplanting mechanism, optimized using the adaptive PSO algorithm, satisfies the trajectory requirements for ship-shaped transplanting.

Acknowledgements

This work was financially supported by Scientific Research Project of Colleges and Universities in Anhui Province (Grant No. 2023AH052645), West Anhui University 2022 High-Level Talent Research Project (Grant No.00701092347) and the Fund of Traditional Chinese Medicine Institute of Anhui Dabie Mountain (TCMADM-2024-16).

[References]

[1] Wan H H, Ren L, Ma J F, Li Y, Xu H R, Yao H J, et al. Sweet potatogibberellin 2-oxidase genes in the dwarf phenotype. Scientia Horticulturae, 2023; 313: 111921.

[2] Xue X L, Li L H, Xu C L, Li E Q, Wang Y J. Optimized design and experiment of a fully automated potted cotton seedling transplanting mechanism. Int J Agric & Biol Eng, 2020; 13(4): 111–117.

[3] Xiao J G, Guan F X, Jiang L, Guang S S, Qing H L, Yu X H. Design and validation of a centrifugal variable-diameter pneumatic high-speed precision seed-metering device for maize. Biosystems Engineering, 2023; 227: 161–181.

[4] Zhao X, Ma X X, Liao H W, Xiong Y S, Xu Y D, Chen J N. Design of flower transplanting mechanisms based on double planet carrier non-circular gear train with complete rotation kinematic pair. Int J Agric & Biol Eng, 2022; 15(3): 9–15.

[5] Niu Z J, Xu Z, Deng J T, Zhang J, Pan S J, Mu H T. Optimal vibration parameters for olive harvesting from finite element analysis and vibration tests. Biosystems Engineering, 2022; 215: 228–238.

[6] Liu Z, Zheng W, Wang N, Lyu Z, Zhang W. Trajectory tracking control of agricultural vehicles based on disturbance test. Int J Agric Biol Eng, 2020; 13(2): 138–145.

[7] Zhang W Z, Zhu Q, Ge D M, Zheng D H, Zhang T T. Design and experiment of the side insertion horizontal transplanting device for sweet potato (*Ipomoea batatas* Lam.) seedlings on mulch film. Int J Agric & Biol Eng, 2023; 16(6): 148–157.

[8] Yang Q, Xu L, Shi X, Ibrar A, Mao H, Hu J, et al. Design of seedlings separation device with reciprocating movement seedling cups and its controlling system of the full-automatic plug seedling transplanter. Comput Electron in Agric, 2018; 147: 131–145.

[9] Wu Y, Gong Z, Chang G, Zhu Y. Design and experiment of type 2ZLF-2 duplex sweet potato transplanter. Agric Equip Veh Eng., 2021; 59(2): 54–57.

[10] Hu L, Wang B, Wang G, Yu Z, You Z, Hu Z, et al. Design and experiment of type 2ZGF-2 duplex sweet potato transplanter. Transactions of the CSAM, 2016; 32(10): 8–16. (in Chinese)

[11] Yin W, Liu H, Hu F, Yan H, Guo D, Wu Y. Optmization design and experiment on eight-linkage planting mechanism of dryland transplanter. Transactions of the CSAM, 2020; 51(10): 51–60. (in Chinese)

[12] Guo K, Lin L S, Li E P, Zhong Y Y, Petersen B L, Blennow A, et al. Effects of growth temperature on multi-scale structure of root tuber starch in sweet potato. Carbohydrate Polymers, 2022; 298: 120136.

[13] Sun L, Shen J H, Zhou Y Z. Design of vegetable pot seedling transplanting mechanism with non-circular gear and connecting rod combination transmission. Transactions of the CSAE, 2019; 35(10): 26–33. (in Chinese)

[14] Tong J H, Qiu Z A, Zhou H L, Bashir M K, Yu G H, Wu C Y, et al. Optimizing the path of seedling transplanting with multi-end effectors by using an improved greedy annealing algorithm. Computers and Electronics in Agriculture, 2022; 201: 107276.

[15] Zheng Z, Li S, Ma J, Wang B, Li C, Cui L. Motion analysis and optimization on cam-link cutting mechanism of fruit-vegetable packaging machine. Transactions of the CSAM, 2016; 47(S1): 374–379. (in Chinese)

[16] Sri M, Hwang S J, Nam J S. Experimental safety analysis for transplanting device of the 4-bar link type semi-automatic vegetable transplanter. Agronomy, 2022; 12(8): 1890.

[17] Zhao X, Zhang X S, Wu Q P, Dai L, Chen J N. Research and experiment of a novel flower transplanting device using hybrid-driven mechanism. Int J Agric & Biol Eng, 2020; 13(2): 92–100.

[18] Wei Y, Hu M J, Li K, Wang J, Zhang W Y. Design and experiment of horizontal transplanter for sweet potato seedlings. Agriculture, 2022; 12(5): 675.

[19] Li M Y, Jin X, Ji J T, Li P G, Du X W. Design and experiment of intelligent sorting and transplanting system for healthy vegetable seedlings. Int J Agric & Biol Eng, 2021; 14(4): 208–216.

[20] Jin X, Cheng Q, Zhao B, Ji J T, Li M Y. Design and test of 2ZYM-2 potted vegetable seedlings transplanting machine. Int J Agric & Biol Eng, 2020; 13(1): 101–110.

[21] Lenaerts B, Aertsen T, Tijskens E, Ketelaere B D, De Ketelaere B, Ramon H, et al. Simulation of grain–straw separation by discrete element modeling with bendable straw particles. Computers and Electronics in Agriculture, 2014; 101: 24–33.

[22] Li L, Xu Y L, Pan Z G, Zhang H, Sun T F, Zhai Y M. Design and experiment of sweet potato up-film transplanting device with a boat-bottom posture. Agriculture, 2022; 12(10): 1716.

[23] Shao Y Y, Zhang H D, Xuan G T, Zhang T, Guan X L, Wang F H. Simulation and experiment of a transplantingmechanism for sweet potato seedlings with‘boat-bottom’transplanting trajectory. Int J Agric & Biol Eng, 2023; 16(3): 96–101.

[24] Qin Y X, Nenad N, Chaminda S R, Nathan M. D’Cunha. Nutrition-related health outcomes of sweet potato (Ipomoea batatas) consumption: A systematic review. Food Bioscience, 2022; 50(3): 102208.

[25] Yang Y M, Cao Hu, Wang Y K, Zhao J B, Ren W Q, Wang B, et al. Non-isocyanate polyurethane from sweet potato residual and the application in food preservation. Industrial Crops and Products, 2022; 186: 115224.

[26] Li H, HE T F, Liu H, Shi S, Zhou J L, Liu X C, et al. Development of the profiling up-film transplanter for sweet potato in hilly and mountainous region. Transactions of the CSAE, 2023; 39(16): 26–35.

[27] Mattar M A, Al-Othman A A, Elansary H O, Elfeky A M, Alshami A K. Field study and regression modeling on soil water distribution with mulching and surface or subsurface drip irrigation systems. Int J Agric & Biol Eng, 2021; 14(2): 142–150.